*J. Fluid Mech.* (1990), *vol.* 213, *pp.* 511–530
*Printed in Great Britain*



# Chaos in a linear array of vortices

By P. TABELING, O. CARDOSO AND B. PERRIN
Groupe de Physique des Solides de l'Ecole Normale Supérieure, 24 rue Lhomond, 75231 Paris, France

(Received 8 July 1988 and in revised form 20 September 1989)

An experimental study of the onset of chaos in a linear array of forced vortices is presented. The vortices are driven by electromagnetic forces in a layer of electrolyte. The system is found to behave like a chain of nonlinearly coupled oscillators, each oscillator being sustained by a pair of vortices. Systems with a small number of vortices exhibit scenarios characterized by a small number of degrees of freedom. Increasing the number of vortices leads to a rapid increase of the complexity of the regimes of transition to chaos. For moderately long systems, quasi-periodicity preceding the onset of chaos and intermittent behaviour is observed.

## 1. Introduction

Dynamical system theory is a powerful tool for describing weak turbulence in confined flows, such as Rayleigh–Bénard convection in a small box (Maurer & Libchaber 1978; Ahlers & Behringer 1979; Bergé & Dubois 1976), Taylor–Couette flow (Fenstermacher, Swinney & Gollub 1979), and others where the instability pattern is strongly constrained geometrically. In such systems, weak turbulence is essentially a temporal chaos, characterized by a small number of degrees of freedom. In contrast, when the cellular flow is poorly confined geometrically, its spatial structure is subjected to chaotic fluctuations and weak turbulence takes the form of spatio-temporal chaos. This type of turbulence is characterized by a large number of degrees of freedom and is still poorly understood theoretically.

Experimental work on spatio-temporal chaos has been performed mostly on convective systems in two distinct situations (for recent papers on the subject, see for instance Gao *et al.* 1987; Kolodner *et al.* 1986; Walden *et al.* 1985; Steinberg, Moses & Fineberg 1987): Rayleigh–Bénard convection in pure fluids, and convection in binary mixtures. In the first situation, the primary instability is in the form of stationary rolls. Spatio-temporal chaos arising slightly above the instability threshold presumably results in this case from the interaction between large-scale flows, local three-dimensional instabilities and pattern defects (see for instance Pocheau, Croquette & Le Gal 1985). Convection in binary mixtures allows study of the case where the first instability sets in as a time-periodic flow (a similar situation can be studied by using the stationary Rayleigh–Bénard convection as the basic state and looking at the dynamics of the oscillatory instability (Croquette & Williams 1989; Chiffaudel, Fauve & Perrin 1989). A great variety of phenomena has been observed prior to the onset of spatio-temporal chaos (formation of localized states, competition between waves, emergence of structure defects). Attempts are made to interpret such phenomena in the framework of an amplitude equation formalism. All these systems are the subject of active research, both theoretical and experimental.

Another system, which gives rise to interesting dynamical behaviour, is obtained

by studying convective instability in an annular geometry and far from the instability threshold (Ciliberto & Bigazzi 1988; Dubois *et al.* 1989). In such experiments, spatio-temporal intermittency is observed, whose features seem to be close to those derived from the Kuramoto–Shivashinsky model (Chaté & Manneville 1986).

The preceding studies have been carried out on patterns which arise from a natural instability. Much less is known on extended patterns produced by forcing. The idea of studying the onset of turbulence in forced periodic flows traces back to Kolmogorov (see Arnol'd & Meshalkin 1960). His basic idea was to impose the scale of injection of the energy and study, as the Reynolds number is increased, how energy is transferred throughout a continuous band of wavenumbers. The model considered by Kolmogorov and further studied by Meshalkin & Sinai (1961), Green (1974) and Sivashinsky (1983) was a plane periodic parallel shear flow. These authors have shown that above a certain threshold, large-scale instabilities develop. In finite-size systems, and after a transient, the system is driven towards a state where only two lengthscales survive, the lattice period and the system size (She 1987; D'Humières 1987). One interesting feature of this model is that the process involved during the transient state seems to be an inverse cascade (Green 1974; She 1987); the geometry of this cascade, which has some link with two-dimensional turbulent cascades, is still the subject of theoretical studies.

Experimentally, the onset of turbulence in spatially periodic flows was first considered by Bondarenko, Gak & Dolzhanskii (1979), by using magnetohydrodynamic forcing. The first instability of the flow was found to lead to a stable stationary supercritical state. The higher-order instabilities were studied only qualitatively. Later on, very interesting results were obtained on two-dimensional periodic flows by Sommeria (1985), and Nguyen Duc & Sommeria (1988). They studied the case of a regular two-dimensional lattice of magnetohydrodynamically forced vortices. Depending on the lattice symmetry, and the boundary conditions, the system evolves towards either a fully developed turbulent state or a spatio-temporal chaos. The nature of the spatio-temporal chaos in this experiment remains to be understood.

In this paper, we present an experimental study of the onset of chaos in a linear array of vortices produced electromagnetically. The flow that we study extends along one direction of space and is confined in the other two, so that the spatial degrees of freedom are trapped in a one-dimensional space. This is a simplification and the results will be compared with other unidimensional systems. We shall follow the evolution of the regimes of transition towards weak turbulence as the size of the lattice is increased and use the simplicity of the physical configuration to provide a quite complete description of various aspects of spatio-temporal chaos for this case.

## 2. Description of the experimental arrangement

The experimental arrangement is shown on figure 1*a*, 1*b*. The cell, 350 mm long, and 35 mm wide, is machined out of Plexiglas. Permanent magnets are located 1.2 mm below the bottom of the cell. They are Samarium Cobalt parallelepipeds, of dimensions $11.2 \times 7 \times 6.5$ mm, and their magnetization axes are vertical. Each magnet produces a magnetic field which has a maximum value of 0.34 T and decays over a typical length of 3 mm. The magnets are put together to form a line of alternated poles. The experimental arrangement allows for the building of such lines with an arbitrary number of magnets, up to 24. The cell is filled partially with a

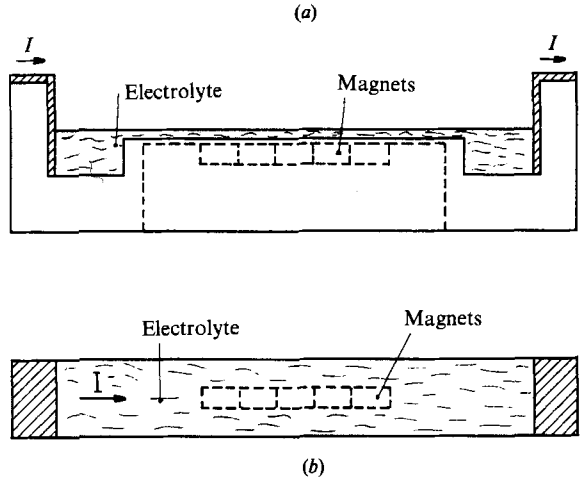


FIGURE 1. The experimental system: (*a*) cross-sectional view; (*b*) top view.

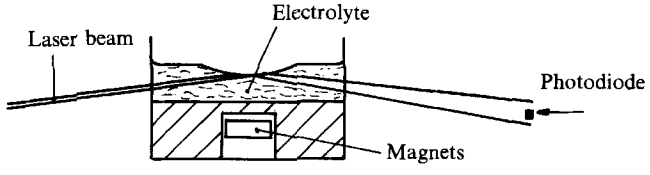


FIGURE 2. Principle of the measurements of the time-dependent evolution of the system.

normal solution of sulphuric acid; the thickness $b$ of the fluid layer is homogeneous along the cell to within $3 \times 10^{-2}$ mm; $b$ is measured with a micrometer, with an accuracy of 0.05 mm.

An electric current $I$, regulated within $10^{-4}$, is driven through the electrolyte, between two copper electrodes, from one side of the cell to the other. The fluid is thus subjected to an electromagnetic force, stationary in time, and periodic in space. In all cases, the period of the forcing is twice the length $\lambda_0$ of a magnet, i.e. 22.4 mm; the magnitude of the forcing is controlled by $I$, which is therefore the control parameter of the experiment.

The flow is studied by using a sheet of light produced by a He–Ne 30 mW laser, and entering laterally just below the free surface with an almost grazing incidence (see figure 2). When we wish to visualize the flow, we put diffusing particles on the free surface. For dynamical studies, the free surface is left clean. We take advantage of the fact that the intensity of the beam reflected under the free surface is very sensitive to the shape of the free surface. The flow induces small deformations, typically of 10 $\mu$m, which thus can be detected by measuring locally, outside the cell, the intensity of the reflected beam. An interesting feature of this method is that when the amplitudes of the temporal modes are small compared with those of the stationary flow, the time-dependent part of the signal is linearly related to the flow disturbance. In the nonlinear regime of detection, the signal keeps track of the frequencies present in the system but is no longer simply related to the disturbance amplitude. Another possibility provided by the optical technique is that *the spatial* structure of the modes of instability can be characterized by phase measurements performed along an axis parallel to the linear array of vortices. We shall use this

information to characterize both the spatial structure and the temporal behaviour of the system.

One source of noise is related to the presence of capillary waves, which are forced by mechanical vibrations present in the environment. Such waves produce a noise whose characteristic frequencies are a few Hz, i.e. about ten times those related to the temporal instabilities of the flow. This noise is minimized by working on an optical table, and filtering out the signal. Another source of noise is the pollution of the free surface; small particles driven on the surface by the flow perturb the reflected beam at frequencies related to the temporal instabilities of the flow. Care is taken to work with clean surfaces. Under those conditions, the signal-to-noise ratio is about 45 dB.

## 3. Summary of the results concerning the stationary states

The stationary states of the flow have been studied previously (Tabeling, Fauve & Perrin 1987) and we summarize herein the main results obtained in the case of large systems, i.e. with a large number of magnets (typically 24). At low currents, the flow is a linear array of counter-rotating vortices of uniform size $\lambda_0$, equal to that of a magnet. This state is stable up to a well-defined value $I_1$, for which we observe the onset of a stationary supercritical instability; above the instability point, the linear array is composed of non-uniform tilted vortices, alternatively big and small. The size difference between two adjacent vortices and the tilt angle are homogeneous throughout the system (except close to the ends); both quantities increase continuously above $I_1$, up to a certain point $I_2$ where half of the vortices shrink. Above $I_2$ (and below the onset of temporal modes), the linear array is composed of steady corotating vortices of sizes $2\lambda_0$. We denote this state as 'state + '.

All these features concern the case where the number of magnets is even. When the number is odd, a defect appears above $I_1$, and the system exhibits time-dependent behaviour just above the instability threshold.

The evolution of the system towards state + has been shown to be related to Kolmogorov instability (Tabeling *et al.* 1987), concerning plane parallel periodic flows (for this instability, see Green 1974). The normal modes of this problem are essentially those responsible for the tilt, and the relative increase of the size of the vortices in our experiment.

## 4. Study of the time-dependent states

### 4.1. *Introduction*

With a large number of magnets, the dynamics of the system turns out to be very complicated, essentially because (as we shall show later) the system behaves like a linear chain of nonlinearly coupled oscillators, each oscillator being sustained by a vortex pair. In view of this behaviour, we first study the case of short linear arrays of vortices, and then follow the evolution of the routes to chaos as the length of the system is increased.

### 4.2. *The case of two corotating vortices*

The case of two corotating vortices is obtained by working with four magnets: in such a configuration, the evolution of the system towards state + is shown in figure 3(*a–c*). At low current, the structure in the central part of the flow is composed of three counter-rotating vortices, a small one squeezed by two large ones (see figure 3*a*). There are also two additional vortices, of much weaker intensity, located at the ends. As $I$ is increased, the small vortex at the centre decreases in size (see figure 3*b*),

and further shrinks to zero (see figure 3*c*); above this point, the stationary states include two large vortices of the same sign in the central region. The evolution of the stationary states from the basic state towards state + in the four-magnet system is thus analogous to that observed in the large system, except that, owing to end effects, there is no sharp transition at $I_1$.

We now have a pair of corotating vortices and investigate the temporal instabilities of this elementary system. The dynamical events observed as $I$ is further increased are shown on figure 3(*d*, *e*). We observe that, above a well-defined threshold $I_c$, both the shape of the vortices and the location of their centres fluctuate with time. Vortices are periodically squeezed, rotate, decrease and so on as time passes. This temporal instability defines a monoperiodic regime, as shown on the power spectrum (see figure 4). Close to the critical point, the amplitude of the oscillation follows a Landau-type law and its frequency is linear with the control parameter, as shown in figures 4–6. The onset of the oscillator thus has the characteristics of a supercritical Hopf bifurcation.

We have studied the dependence of threshold $I_c$ and frequency $f_c$ at onset with thickness $b$ of the fluid layer; the results are shown on figure 7. There are two regimes: at small $b$, the following experimental laws are observed:

$$I_c \approx 160b^{-3} \quad \text{and} \quad f_c \approx 650b^{-2},$$

where $b$, $I$ and $f$ are measured in mm, mA and mHz respectively.

These scaling laws can be understood by the following arguments similar to those developed in a preceding paper (Tabeling *et al.* 1987): at small values of $b$, the flow is two-dimensional and the velocity profile along the normal to the bottom of the cell is close to a parabola; in this regime, the fluid viscosity $\mu$ enters the problem only through the product $\mu/b^2$, and, by using dimensional arguments, we deduce that the system is entirely governed by a Reynolds number whose expression is

$$Re = \rho B_0 I b^3/\mu^2 w^2,$$

in which $\rho$ is the mass density, $B_0$ is a characteristic value for the magnetic field, and $w$ is the width of the cell. This shows that $Ib^3$ is a constant at the instability threshold, which is precisely what we observe; the corresponding value of the Reynolds number (obtained by replacing $B_0$ by its maximum value, i.e. 0.34 T), is $Re_c \approx 45$. Similarly, we define the Strouhal number of the system as

$$S = fw^2\mu/B_0 Ib = fb^2/\nu Re,$$

in which $f$ is the frequency of the temporal mode and $\nu$ the kinematic viscosity. The fact that $fb^2$ is a constant at onset shows that there is a critical value for $S$, which we find equal to approximately $1.4 \times 10^{-2}$. These results indicate – indirectly – that the range of small $b$ is associated to a two-dimensional regime of flow.

As $b$ is increased above 2.5 mm, more complicated dependence of $I_c$ and $f_c$ is observed (see figure 7); this defines a second regime of flow in which presumably three-dimensional effects, such as those related to the presence of secondary flows, cease to be negligible. The flow is still essentially two-dimensional in a kinematical sense but dynamically, three-dimensional effects become relevant as soon as $b$ is larger than 2.5 mm.

The physical origin of the oscillation is related to a shear instability which develops from the region between the two vortices; by using a video camera, we have estimated the critical values of the local Reynolds number $Re_1 = \rho G\delta^2/\mu$ (where $G$ is the velocity gradient and $\delta$ is the size of the shear region). The typical values that we

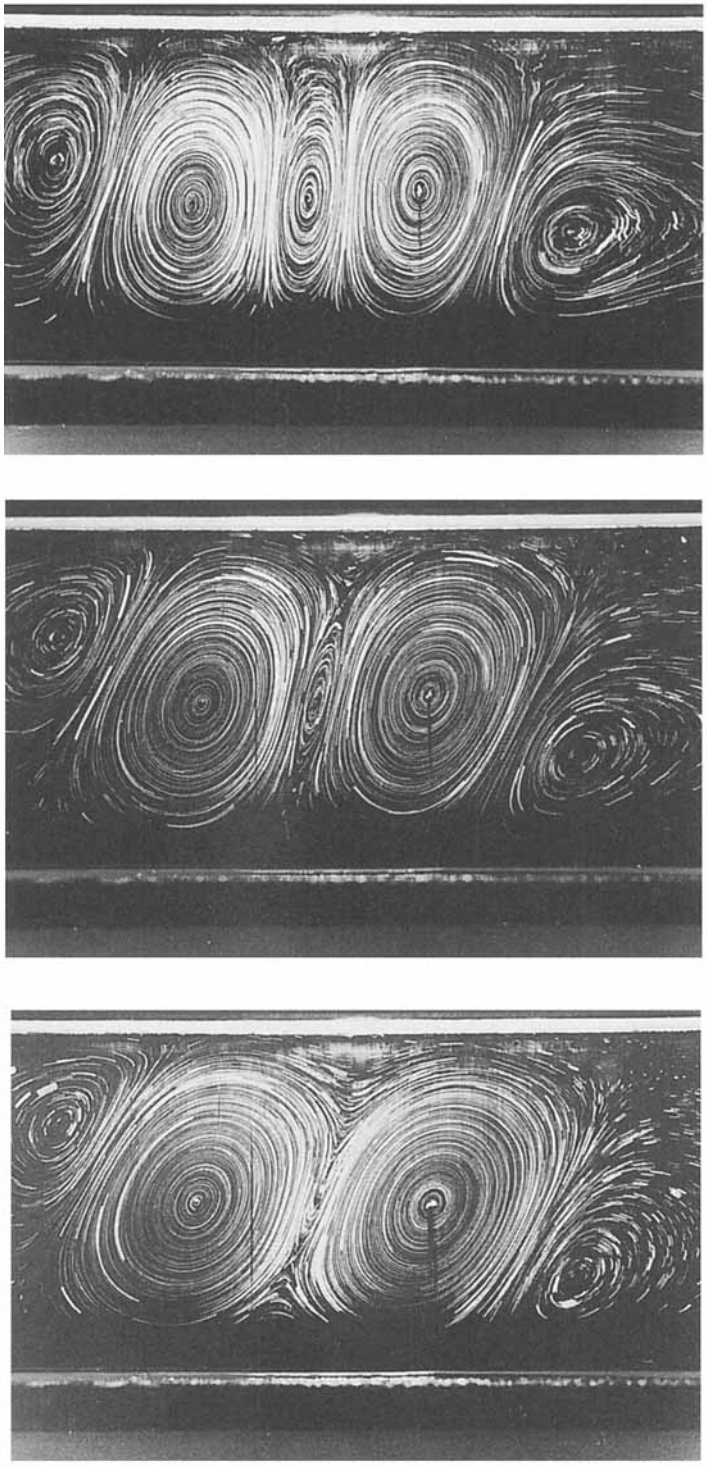


FIGURE 3(a–c). For caption see facing page.

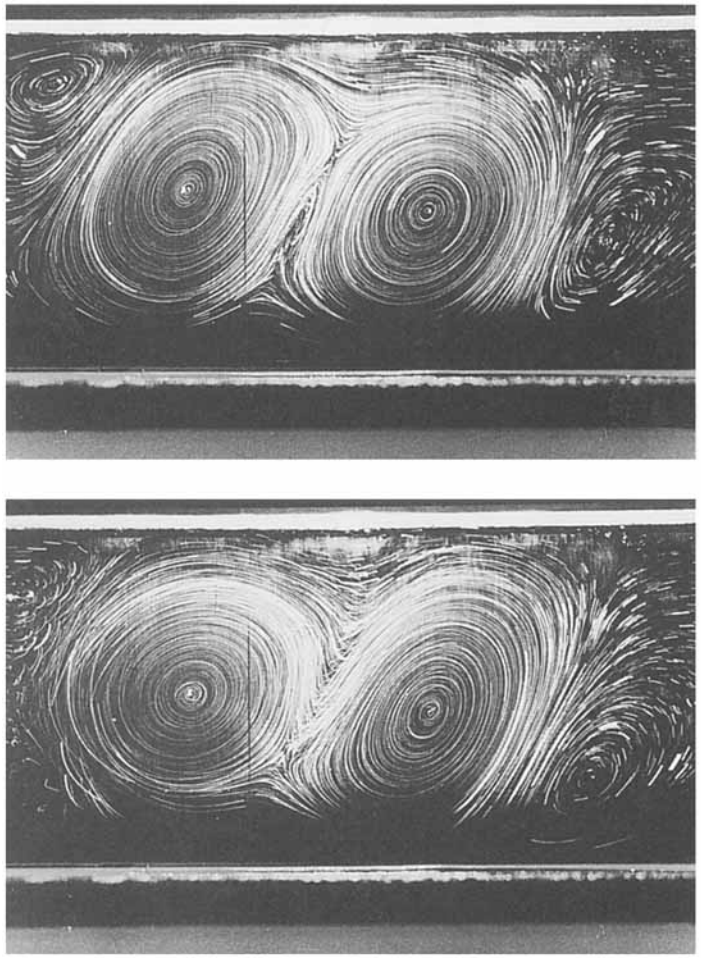


FIGURE 3. Different states of flow for the case of four magnets, for $b = 2.50$ mm and for various values of $I$; (*a*) $I = 4.93$ mA; (*b*) 10.81 mA; (*c*) 13.09 mA; (*d*) 20.84 mA; (*e*) 24.75 mA.

find are 50; such values are consistent with theoretical estimates for the onset of shear instability in a dissipative situation (Chomaz 1986) – similar to that which we study. This shear instability produces a distortion of the streamlines, which is advected by the vortices at a rate close to that relative to the mean rotation of the vortex.

In order to characterize the spatial structure of this oscillation, we have performed phase measurements. Figure 8 shows the phase shift of the time-periodic signal between two optical probes located at positions corresponding to the centres of the vortices. We have checked, by visual observation, that this measurement characterizes the spatial oscillation of the vortex centres. We obtain the same phase difference – equal to 180° – throughout the supercritical range, except very close to $I_c$. By analogy with vibration modes in crystals (although in this case the 'crystal' is very short), we call this mode 'optical'. The spatial structure of the oscillation is found to be independent of the fluid thickness.

The range of stability of the oscillation is quite large: it extends from $I_c$ to typically $3I_c$. At larger values of $I$, the system undergoes a sequence of subharmonic

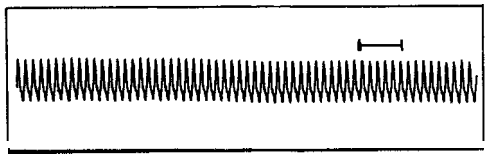

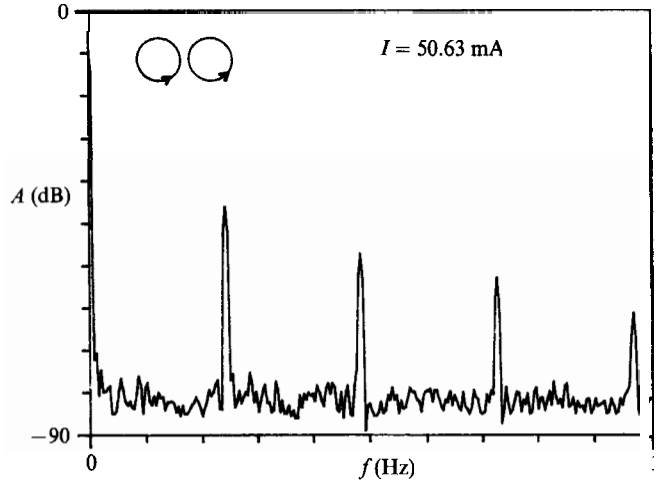


FIGURE 4. Direct time recording and Fourier spectrum of the signal obtained on a detector, for the case of four magnets, for $n = 2.61$ mm.

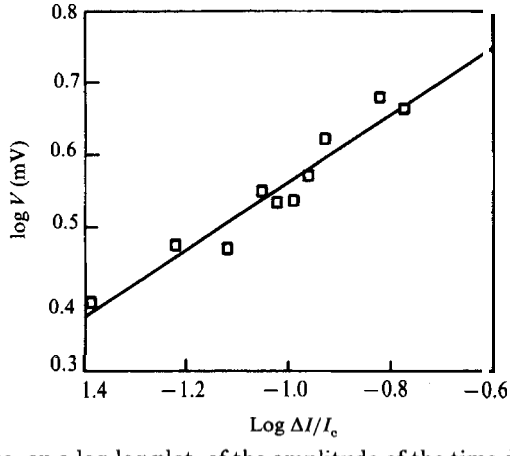


FIGURE 5. Dependence, on a log-log plot, of the amplitude of the time dependent mode on the ratio of $\Delta I$ to the critical point $I_c$, (where $\Delta I = I - I_c$) for the four-magnet case, with $b = 2.11$ mm. In this experiment, $I_c$ is 18.45 mA. The straight line has a slope equal to 0.5.

instabilities leading to chaos, as shown in figure 9. We usually observe the presence of a one-third subharmonic preceding the onset of chaos, and we have not been able to observe more than one subharmonic bifurcation. The fact that chaos is observed just above subharmonic generation and that the Fourier spectrum in the chaotic regime shows broad bands centred on the main frequency and its subharmonics

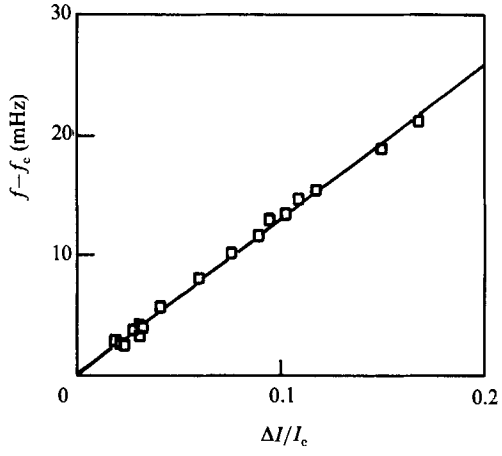


FIGURE 6. Variation of the quantity $f-f_c$ with $\Delta I/I_c = (I-I_c)/I_c$, for the case of four magnets, with $b = 2.11$ mm. In this experiment, $f_c = 148.5$ mHz.

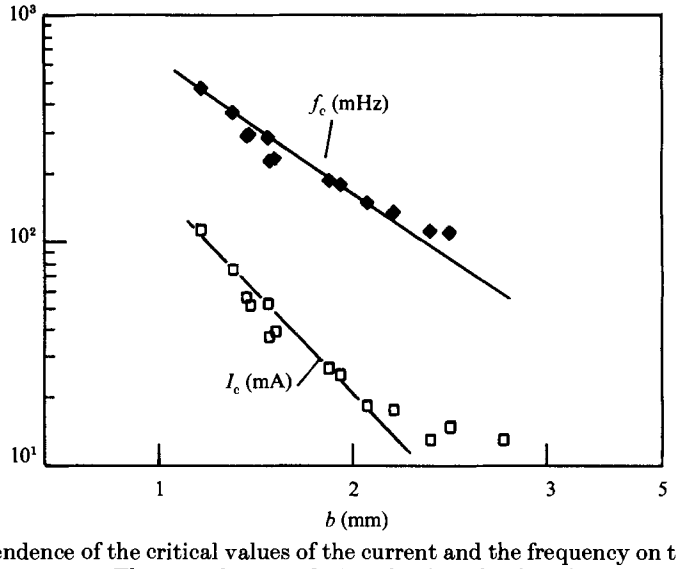


FIGURE 7. Dependence of the critical values of the current and the frequency on the fluid thickness, for the four-magnet case. The straight lines fitting the data for $f_c$ and $I_c$ have slopes $-2$ and $-3$ respectively.

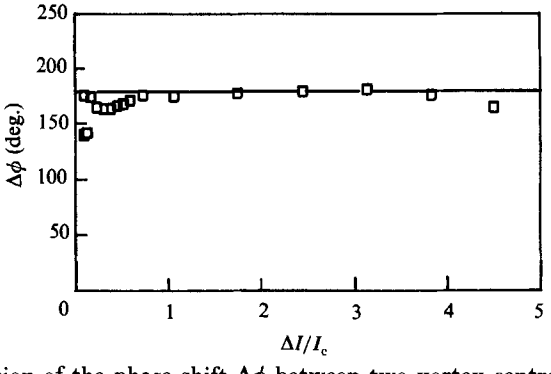


FIGURE 8. Evolution of the phase shift $\Delta\phi$ between two vortex centres with current $I$ in the supercritical regime of flow, for the case of four magnets, with $b = 2.5$ mm.

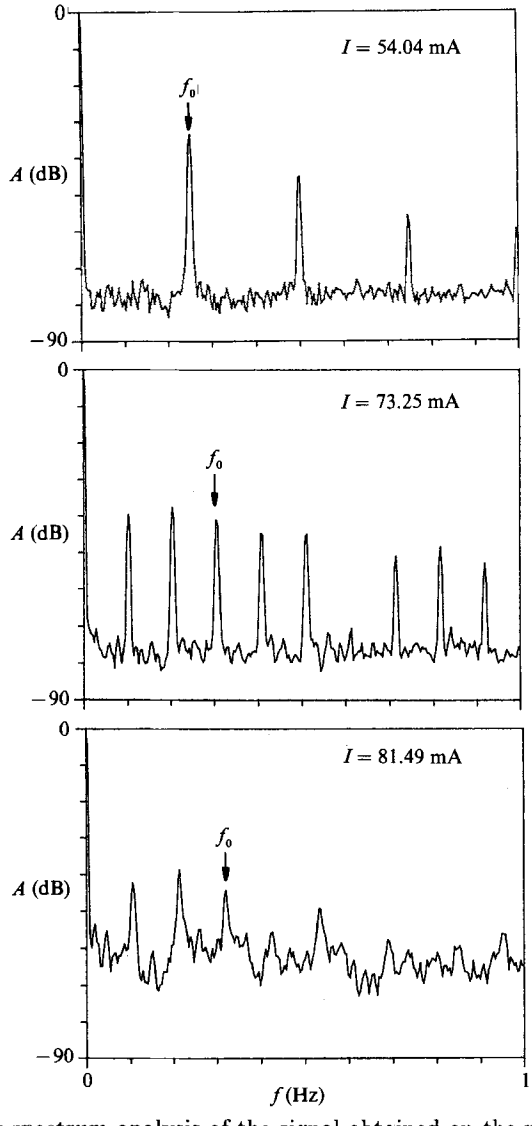


FIGURE 9. Power spectrum analysis of the signal obtained on the photodiodes for different values of $I$, for the case of four magnets, with $b = 2.50$ mm.

indicate that the onset of chaos is related to a low-dimensional scenario, such as a subharmonic cascade.

The evolution towards chaos for the pair of corotating vortices is thus simple. There is a single 'oscillator' present in a nonlinear system, which drives the flow to chaos by generating subharmonics instabilities. We recover in this case the well-known evolution of a strongly confined system dominated by a single oscillator.

### 4.3. *The case of three corotating vortices*

Three corotating vortices are the 'state +' for a system with six magnets. In this case, the spatial structure of the flow at low values of $I$ is composed of five counter-rotating vortices – three large and two small – in the central region. Similarly to the four-magnets case, as the control parameter $I$ is increased, the two small vortices

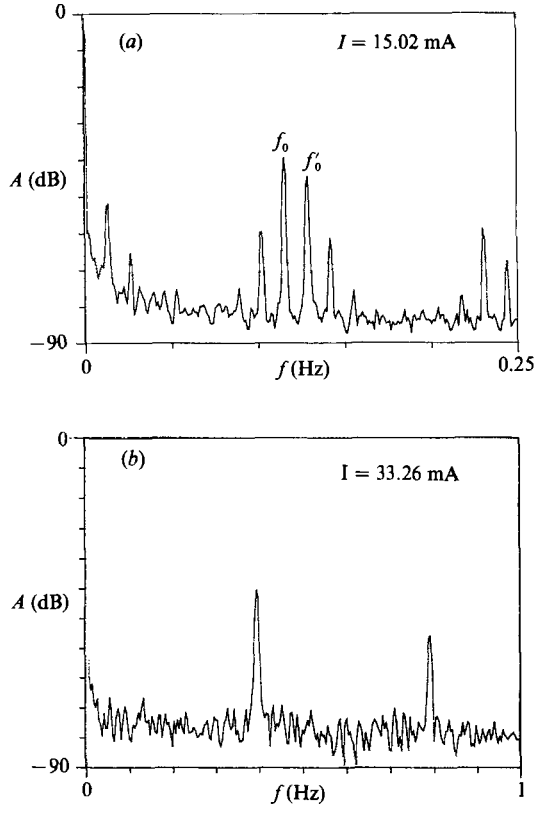


FIGURE 10. Power spectra obtained for the case of six magnets, for $b = 2.50$ mm, and different values of $I$.

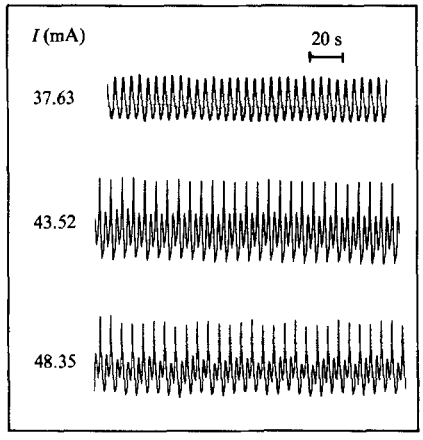


FIGURE 11. Onset of chaos for the six-magnet case, for $b = 2.50$ mm. The state for $I = 48.35$ mA is chaotic; for this value of $I$, one can see the presence of subharmonics up to $\frac{1}{8}f_0$.

decrease in size while the others increase; above a well-defined value of $I$, the central region of the system involves only three vortices of the same sign, defining the 'state + '. There are now two regions of large shear, located between each pair of vortices; above a new threshold $I_c$, which is close to that found in the four-magnets case, for the same value of $b$, state + is subjected to temporal instability. Figure 10(*a*) shows

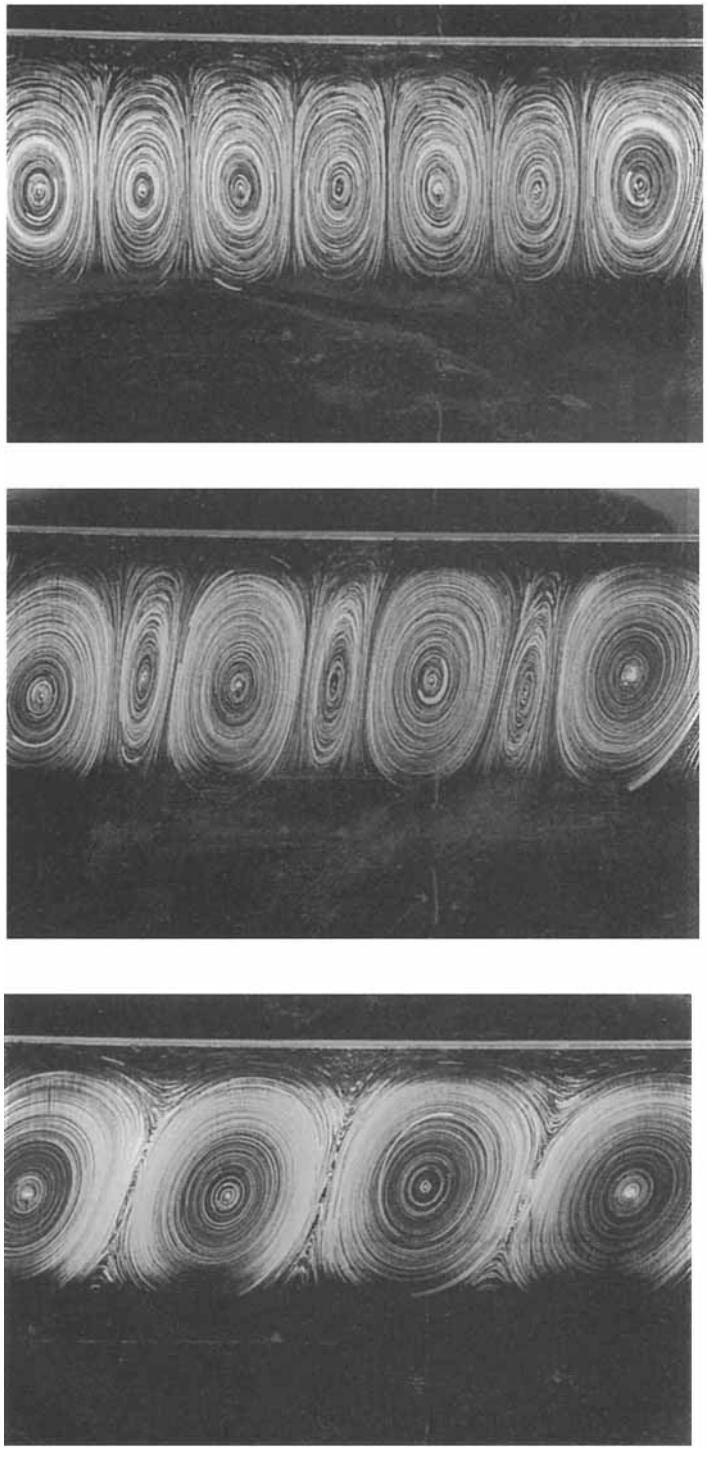


FIGURE 12(a–c). For caption see facing page.

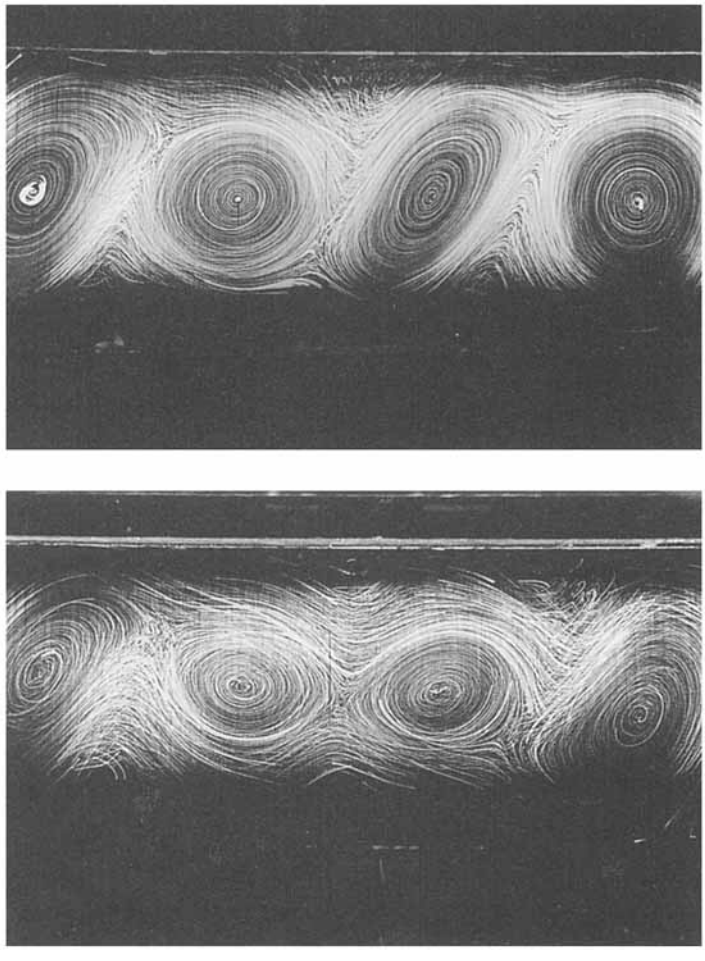


FIGURE 12. Different state of flow for the case of eight magnets, for $b = 2.10$ mm and for various values of $I$; (*a*) $I = 3.68$ mA; (*b*) 13.94 mA; (*c*) 22.77 mA; (*d*) 32.60 mA; (*e*) 50.13 mA.

that Fourier spectrum of the signal, obtained on the photodiode, for $I = 15.02$ mA, for the case where $b = 2.50$ mm. This value of $I$ corresponds to a point just above $I_c$. There are two distinct oscillators – $f_0$ and $f_0'$ – whose frequencies are very close to each other: we find 117.2 mHz for the first oscillator and 129.1 mHz for the second one (see figure 10*a*). As $I$ is further increased, the two frequencies lock in (see figure 10); the lock-in state remains stable over a wide range of values of the control parameter, extending typically from $I_c$ to $2I_c$ or $3I_c$. This state is them subjected to subharmonic instability, preceding the onset of chaos (see figure 11).

As with two corotating vortices, the physical origin of $f_0$ and $f_0'$ is related to a shear instability originating between each pair of vortices. The main arguments for this statement are that, visually, the mode of instability looks very similar to that observed in the corotating vortex pair; moreover, the observed thresholds and frequencies are very close to those found in the two corotating vortices system. In the three-vortices case, there are two regions of high shear so that the dynamics of the system is controlled by two almost identical oscillators. The fact that, close to the threshold, two distinct frequencies are observed might be due either to small

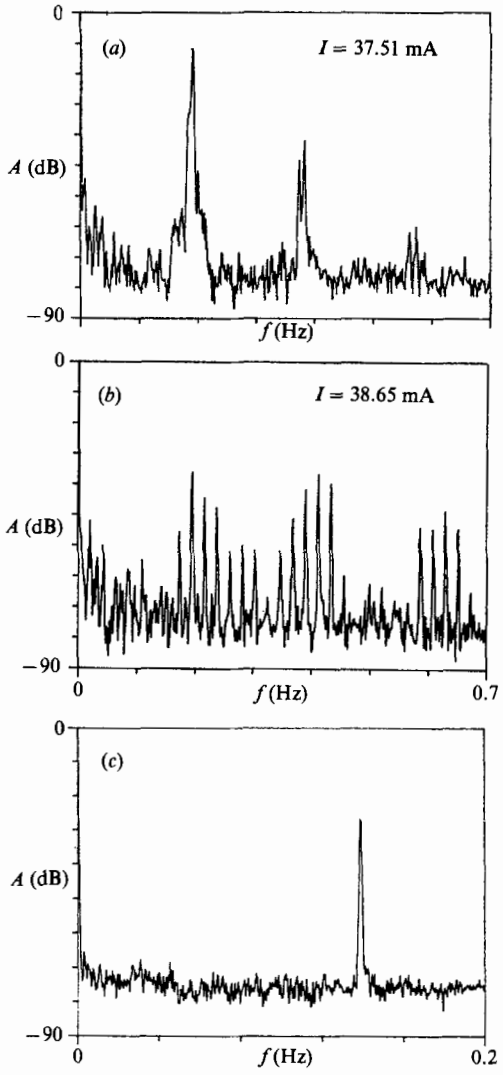


FIGURE 13. Power spectra obtained for the case of eight magnets, for various values of $I$, with $b = 1.5$ mm.

imperfections in the experimental system, or to the existence of a linear coupling between the two oscillators (which would give rise to a splitting effect from the natural frequencies of the basic oscillators). The nonlinear coupling between them manifests itself in the existence of a frequency lock-in state at larger values of the control parameter. The fact that the onset of chaos is related to period doubling shows that the dynamics of the system remains trapped in a space of low dimensionality.

These results show that the three corotating vortices system is again essentially a strongly confined system but now dominated by two oscillators.

### 4.4. *Onset of intermittency in the four-vortices system and above*

Figure 12(*a–c*) summarizes the evolution of the system towards state + in the case of eight magnets, and for $b = 2.10$ mm. At low current, there are eight counter-

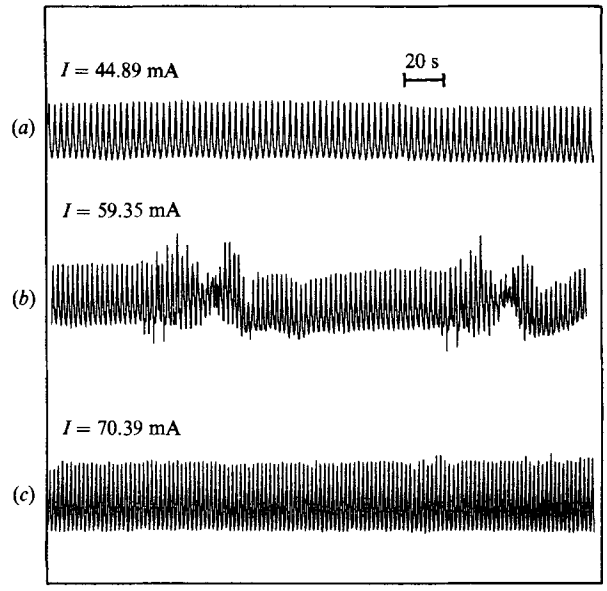


FIGURE 14. Typical direct time recordings showing the onset of intermittency for the case of eight magnets.

rotating vortices in the central region (see figure 12*a*); as $I$ is increased, some of the vortices decrease in size whereas the others increase (see figure 12*b*); finally, the flow evolves towards a four-corotating vortex state shown in figure 12(*c*). There are now three regions of high shear. As $I$ is further raised, we first observe a chaotic state (see figure 13*a*). The threshold value for the onset of this temporal event is close to the previous critical values $I_c$ (see §4.2). This chaotic state is presumably the signature of the existence of three basic oscillators in weak nonlinear interaction, which, according to the general prediction of Ruelle & Takens (1971), would lead to a chaotic state. However, in the present experiment, the size of the chaotic region – in the parameter space – is too small to be studied accurately; it is thus difficult to make precise inferences concerning such a chaotic regime.

As $I$ is increased again, the regime ceases to be chaotic and a quasi-periodic state is observed (see figure 13*b*). We then have a 'partial' lock-in state. The subsequent regime is a 'complete' locking state, leading to a monoperiodic oscillation (see figure 13*c*). In this regime, the temporal instability has a remarkable spatial structure, characterized by the fact that each vortex is out of phase with the next one (see figure 12*d*). This is the optical mode previously found in the four-magnet system (see §4.2). The spatial structure of this mode remains stable within a range extending approximately from $I_c$ to $2I_c$ ($I_c$ is about 19 mA for $b = 2.11$ mm).

A new dynamical event is detected above a new threshold value for $I$, denoted by $I_s$, where we observe the onset of intermittency on the optical detectors, as shown on figure 14: the value of $I_s$ is in this case about 40 mA; below $I_s$, the regime is monoperiodic and the system is locked on the optical mode (figure 14*a*); above $I_s$, the signal is composed of monoperiodic phases, separated by bursts (figure 14*b*); the mean duration of the monoperiodic phases first decreases with $I$ and then increases again; For $I$ far above $I_s$, the system is again monoperiodic (see figure 14*c*).

The spatial structure of the flow far above $I_s$ is shown on figure 12*e*, for $I =$ 50.13 mA. It looks very different to that below $I_s$ (see figure 12*d*): in the present case,

we observe that the two central vortices roughly oscillate in phase, as do two extreme ones, and there is a large phase shift between the end vortices and the central ones. This structure is confirmed by the phase measurements. We find a small phase difference of about 10° to 30° between the two central vortices, a similar phase difference between the two extreme ones, and a phase shift roughly equal to 180° between these two groups of vortices. Although it is difficult to interpret a structure in so small a system, it can be seen as describing two travelling waves originating from the centre of the system and propagating along the lattice in opposite directions with about the same phase velocity. We call this mode the 'counter-propagating mode'. This structure is very different to that of an optical mode, and it turns out that the system undergoes a first-order transition from one structure to the other as the control parameter is increased. The signature of this spatial transition in the dynamical space is a regime of competition between two limits cycles, leading to intermittency.

The range of stability of the counter-propagating mode extends to abut $4I_c$. At larger values of $I$, this mode is subjected to subharmonic instabilities which further trigger the onset of temporal chaos. We recover, in this case, the dynamical behaviour of the two- and three-vortex systems at large values of the control parameter.

The main novelty in the four-vortex state is therefore the existence of a phase transition between two spatial modes, denoted respectively as optical and counter propagating. In this relatively short system, we already have dynamical events related to the fact that the linear array can sustain distinct spatial structures. The dynamics of the system no longer reduces to that of a single oscillator.

### 4.5. *The case of a larger number of corotating vortices, up to* 12

When we increase the number of corotating vortices, the number of regions of large shear increases, giving rise to the onset of a larger number of oscillators above $I_c$; we thus expect to find an increasing complexity of the regimes of flow preceding the onset of chaos. We have studied configurations with different numbers of magnets, from 10 up to 24. The results shown below have been obtained for the case of 16 magnets; they are typical (but not exhaustive) of the regimes found for reasonably large systems.

The results found in the 16-magnet case, for which state + is a linear array of eight corotating vortices, are summarized in the phase diagram shown in figure 15. Surprisingly, we find a sensitive dependence of the behaviour of the system on the depth of the fluid layer $b$, so that the phase diagram includes both $I$ and $b$ as parameters. Such a dependence of the regimes on $b$ is not observed in small systems, i.e. when the number of corotating vortices is smaller than six.

There are two regions in the phase diagram. When $b$ is larger than 2.9 mm (and below 4 mm), we invariably observe the following sequence of events as the control parameter is increased from state + : chaotic quasi-periodic with two frequencies, monoperiodic, and then intermittency leading to chaos.

The observation of chaos just above state + can be interpreted as related to the presence of many oscillators interacting nonlinearly. Such oscillators lock-in 'partially' in the form of a quasi-periodic state. The 'complete' lock-in state is observed at larger values of $I$, in the form of a monoperiodic state, with a well-defined frequency, and whose domain of stability is quite large (see the phase diagram). By using a video camera, and phase measurements, we observe that the corresponding spatial structure of this regime is an optical mode. As $I$ is further increased, the direct

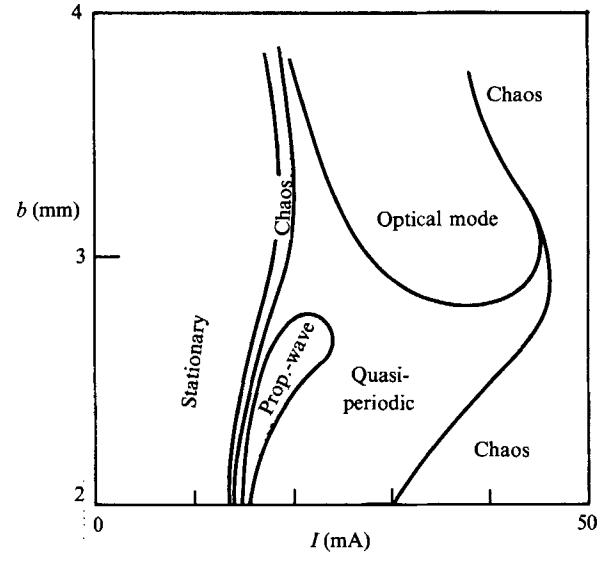


FIGURE 15. Phase diagram of the 16-magnet system.

time recordings on the optical detectors show the onset of intermittency, which persists and increases at larger values of the control parameter. Outside the boundary of the optical 'tongue' of the system, we thus observe intermittent behaviour, which turns out to be the particular form of chaos observed in this region of the phase diagram.

It is plausible that the chaotic regime is related to a crisis between limit cycles in the phase space. Below the onset of intermittency, the lattice sustains a stable optical mode, which we know to lose stability as the control parameter is increased (see §4.4). In short systems, the system undergoes a transition towards stable counter-propagating waves: this has been observed for four up to six corotating vortices. In contrast, we did find a situation where such stable states exist when the size of the linear array is larger. This can be a direct consequence (in no way easy to understand) of the decrease of the confinement on particular collective modes of oscillation, which remain to be identified in large systems.

Another sequence of events is observed for small values of the thickness of the fluid layer: for $b < 2.75$ mm, we observe the following succession of dynamical events as $I$ is increased from 'state +': chaotic, quasi-periodic, monoperiodic, quasi-periodic and finally chaotic. In contrast with the regimes described above, the range of stability of the complete locking state is very narrow: it extends from $I_c$ to typically $1.05I_c$. Phase measurements and visual observation indicate that the spatial structure of this mode is in the form of a travelling wave. The transition from this state to the quasi-periodic regime is continuous. Above a well-defined value $I_d$ of the control parameter, which we call the 'desynchronization threshold', a new sharp peak appears in the spectrum, close to the main one; its amplitude increases with $I$ and then saturates at a level comparable to that of the first frequency. This transition, which is reversible, thus corresponds to the evolution of the system from a 'complete locking state' towards an 'incomplete locking state', where two distinct frequencies are present. Subsequently in the phase diagram, for much larger values of the control parameter, the system becomes chaotic.

We thus observe at small values of $b$, a phenomenon of desynchronization of the

chain of oscillators. We do not observe such a phenomenon when the number of corotating vortices is smaller than five. One can note that the geometrical non-uniformities of the cell are enhanced when both $b$ is decreased and the length of the system is increased. Since the frequency of the oscillators is very sensitive to the value of $b$, geometrical non-uniformities can have a significant effect on the dynamical behaviour of the system; in particular they can favour desynchronization. However, this does not explain why the system first locks in a monoperiodic state, and further, under the increase of the control parameter, undergoes a second-order transition towards quasi-periodicity. Such an evolution may suggest that the linear chain of oscillators is structurally unstable in this region of the phase diagram.

The two regions of the phase diagram are separated by a 'channel' where no 'complete' lock-in state is observed: the system evolves from chaos to quasi-periodicity and from there to chaos without encountering monoperiodic regimes.

## 5. Discussion and conclusions

The results of this study indicate that, dynamically, the system behaves like a linear chain of oscillators. As the number of vortices increases, the system shows a more complex behaviour which may correspond to the fact that it evolves in a phase space of increasing dimension. Complexity has already appeared for eight corotating vortices and preliminary results obtained on larger arrays indicate that it increases further with the size of the system.

There are not many theoretical studies of this type of system. In the work of Fujisaka & Yamada (1982, 1985), the coupling between the oscillators extends throughout the lattice, and its strength is characterized by a parameter $D$. For large $D$, they observed a homogeneous synchronized state, where all the oscillators are in phase. This state becomes unstable as $D$ is decreased, leading to quasi-periodic or chaotic behaviour. An equivalent of $D$ in our experiment may be the control parameter, since the coupling of the oscillators presumably increases with the Reynolds number. We thus observe something analogous to what they find in the lower range of the values of the control parameter, although in our experiment the synchronized state has not the same spatial structure. It would indeed be interesting to proceed to a more detailed comparison with such models.

Another interesting comparison can be done with the theoretical results of She (1987). He determined numerically the transition regimes towards turbulence in the Kolmogorov system. He found several features that we observe, i.e. quasi-periodic states preceding the onset of chaos and intermittent behaviour. It is interesting to note that in spite of the fact that the viscous dissipation in his model is very different from that in the experiment, similarities exist in the dynamical behaviour for both systems.

From the experimental point of view, it is interesting to compare our results to those obtained by Sommeria (1986) concerning two-dimensional arrays of counter-rotating vortices. In this system, two possibilities can arise depending on the spatial symmetries of the lattice and the boundary conditions: for square systems, or hexagonal systems in a circular container, the first instability is the pairing mode, which turns out to be a precursor for the inverse energy cascade. In contrast, for hexagonal lattices with hexagonal walls, the pairing mode is inhibited. In this case, the system sustains propagating waves, with wavelengths related to the lattice period. Chaos may arise from the interaction of several waves in the system; this behaviour has some similarities with the one observed in our experiment, since in

both cases, the lattice sustains oscillations, the major difference lying in the way that such oscillations become unstable. In our system, the dynamics is dominated by competition between various modes of oscillations – leading to intermittency; in the two-dimensional lattice, one may ask if different modes can coexist, and if their mutual interaction can drive the system to chaos. It would be interesting to pursue such comparisons and analyse the behaviour of the two systems in more general terms.

It is interesting to point out that a particular type of convective linear system (Ciliberto & Bigazzi 1988; Dubois *et al.* 1989) shows similarities with our experiment, in the sense that in both cases intermittency is observed when the number of basic cells becomes reasonably large. Indeed in our experiment, we have focused on the problem of the identification of the basic oscillation, its coupling with its neighbours, and the main features of the collective modes; it would be interesting now to perform quantitative measurements on the intermittent regimes and compare with theoretical models for spatio-temporal intermittency.

The present research was supported by DRET Grant no. 86/1512/DRET/DSDR. The authors acknowledge A. Chiffaudel, P. Hohenberg, D. Bensimon, H. Brand, V. Croquette, F. Daviaud, K. Sawada for very fruitful discussions.

## REFERENCES

Ahlers, G. & Behringer, R. 1978 Evolution of turbulence from the Rayleigh–Bénard instability. *Phys. Rev. Lett.* **40**, 712–716.

Arnol'd, V. I. & Meshalkin, L. D. 1960 The seminar of A. N. Kolmogorov on selected topics in analysis (1958–1959). In *Usp. Mat. Nauk* **15**, 247.

Bergé, P. & Dubois, M. 1976 Time dependent velocity in Rayleigh–Bénard convection: a transition to turbulence. *Opt. Comm.* **19**, 129–133.

Bondarenko, N., Gak, M. & Dolzhanskii, F. 1979 *Izv. Akad. Nauk SSSR Ser. Fiz Atmos. i Okeana* **15**, 1017.

Chaté, H. & Manneville, P. 1986 Transition to turbulence via spatio-temporal intermittency, *Phys. Rev. Lett.* **58**, 112.

Chiffaudel, A., Fauve, S. & Perrin, B. 1989 Spatio-temporal dynamics of oscillatory convection at low Prandtl number: waves and defects. *Phys. Rev.* A (to appear).

Chomaz, J. M. 1985 Etude expérimentale et numérique d'une zone cisaillée circulaire: caractérisation des transitions entre modes. Thèse, Univerité Pierre et Marie Curie, Paris.

Ciliberto, S. & Bigazzi, P. 1988 Spatiotemporal intermittency in Rayleigh–Bénard convection. *Phys. Rev. Lett.* **60**, 286–289.

Croquette, V. & Williams, H. L. 1989 Nonlinear competition between waves on convective rolls. *Phys. Rev.* A (to appear).

Dubois, M., Da Silva, R., Daviaud, F., Bergé, P. & Petrov, A. 1989 Collective oscillating mode in a one dimensional chain of convective rolls. *Europhys. Lett.* **8**, 135.

Fenstermacher, P. R., Swinney, H. L. & Gollub, J. P. 1979 Dynamical instabilities and the transition to chaotic Taylor vortex flow. *J. Fluid Mech.* **94**, 103–128.

Fujisaka, H. & Yamada, T. 1982 Stability theory of synchronized motion in coupled-oscillator systems II. *Prog. Theor. Phys.* **69**, 32–47.

Fujisaka, H. & Yamada, T. 1985 Stability theory of synchronized motion in coupled-oscillator systems IV. *Prog. Theor. Phys.* **75**, 1087–1104.

Gao, H., Metcalfe, G., Jung, T. & Behringer, R. P. 1987 Heat flow experiments in liquid $^4$He with a variable cylindrical geometry. *J. Fluid Mech.* **174**, 209–231.

Green, J. S. A. 1974 Two-dimensional turbulence near the viscous limit. *J. Fluid. Mech.* **62**, 273–287.

Kolodner, P., Bensimon, D. & Surko, C. M. 1988 Travelling-wave convection in an annulus. *Phys. Rev. Lett.* **60**, 1723–1726.

KOLODNER, P., PASSNER, A., SURKO, C. M. & WALDEN, R. W. 1986 Onset of oscillatory convection in a binary fluid mixture. *Phys. Rev. Lett.* **56**, 2621.

KURAMOTO, Y. 1984 *Chemical oscillations, waves and turbulence*. Springer.

MAURER, J. & LIBCHABER, A. 1979 Rayleigh–Bénard experiment in liquid helium: frequency locking and the onset of turbulence. *J. Phys. Lett.* **40**, L419–L423.

MESHALKIN, L. D. & SINAI, YA. G. 1961 Investigation of the stability of the stationary solution of a system of plane motion equations of a viscous incompressible fluid. *Prikl. Mat. Mekh.* **25**,

NGUYEN DUC, J. M. 1988 Instabilité et turbulence dans des écoulements bidimensionnels MHD. Thèse, INPG, Grenoble.

NGUYEN DUC, J.-M. & SOMMERIA, J. 1988 Experimental characterization of steady two-dimensional vortex couples. *J. Fluid Mech.* **192**, 175–192.

POCHEAU, A., CROQUETTE, V. & LE GAL, P. 1985 Turbulence in a cylindrical container of argon near threshold convection. *Phys. Rev. Lett.* **55**, 1094–1097.

POMEAU, Y. & MANNEVILLE, P. 1979 Stability and fluctuations of a spatially periodic convective flow. *J. Phys. Lett.* **40**, L609.

RABAUD, M. & COUDER, Y. 1983 A shear flow instability in a circular geometry. *J. Fluid Mech.* **136**, 291–319.

RUELLE, D. & TAKENS, F. 1971 On the nature of turbulence, *Commun. Math. Phys.* **20**, 167–192.

SHE, Z. 1987 Instabilités et dynamique à grande échelle en turbulence. *Thèse, University of Paris* 7.

SIVASHINSKY, G. I. 1983 Negative viscosity effect in large-scale turbulence; long-wave instability of a periodic system of eddies. *Phys. Lett.* **95A**, 152.

SIVASHINSKY, G. 1985 Weak turbulence in periodic flows. *Physica* **17D**, 243–255.

SOMMERIA, J. 1986 Experimental study of the two-dimensional inverse energy cascade in a square box. *J. Fluid Mech.* **170**, 139–168.

STEINBERG, V., MOSES, E. & FINEBERG, J. 1987 Spatio temporal complexity at the onset of convection in a binary fluid. In *The physics of Chaos and Systems far from Equilibrium* (ed. M. Duong Van & B. Nichols.) *Nucl. Phys. B (Proc. Suppl.)*.

TABELING, P., FAUVE, S. & PERRIN, B. 1987 Instability of a linear array of forced vortices. *Europhys. Lett* **4**, 555–560.

WALDEN, R. W., KOLODNER, P., PASSNER, A. & SURKO, C. M. 1985 Traveling waves and chaos in convection in binary fluid mixtures. *Phys. Rev. Lett.* **55**, 496–499.